Uniaxial versus hydrostatic pressure-induced phase transitions in $CaFe_2As_2$ and $BaFe_2As_2$

Milan Tomić, Roser Valentí, and Harald O. Jeschke
Institut für Theoretische Physik, Goethe-Universität Frankfurt, Max-von-Laue-Straße 1, 60438 Frankfurt am Main, Germany
(Received 28 June 2011; revised manuscript received 25 January 2012; published 16 March 2012)

We present *uniaxial* pressure structural relaxations for $CaFe_2As_2$ and $BaFe_2As_2$ within density functional theory and compare them with calculations under hydrostatic pressure as well as available experimental results. We find that $CaFe_2As_2$ shows a unique phase transition from a magnetic orthorhombic phase to a nonmagnetic collapsed tetragonal phase for both pressure conditions and no indication of a tetragonal phase is observed at intermediate uniaxial pressures. In contrast, $BaFe_2As_2$ shows for both pressure conditions two phase transitions from a magnetic orthorhombic to a collapsed tetragonal phase through an intermediate nonmagnetic tetragonal phase. We find that the critical transition pressures under uniaxial conditions are much lower than those under hydrostatic conditions manifesting the high sensitivity of the systems to uniaxial stress. We discuss the origin of this sensitivity and its relation to experimental observations.

DOI: 10.1103/PhysRevB.85.094105 PACS number(s): 74.70.Xa, 61.50.Ks, 71.15.Mb, 64.70.K−

I. INTRODUCTION

The discovery of superconductivity in iron pnictides[1] has initiated an enormous amount of activities related to these materials. Superconductivity can be triggered either by chemical doping or by application of pressure on the undoped parent compounds. One of the families that has been intensively studied under pressure is the 122 family $AEFe_2As_2$ (AE = Ca, Sr, and Ba). $CaFe_2As_2$ at ambient pressure undergoes a first-order phase transition from a tetragonal to an orthorhombic phase at 172 K accompanied by a magnetic transition. Initial reports on pressure experiments showed that at $P \sim 0.23$ GPa the orthorhombic and antiferromagnetic phases are suppressed and the system superconducts at low temperatures.[2,3] Moreover, a compressed tetragonal phase—also called "collapsed" tetragonal phase—was identified at higher pressures. Subsequent susceptibility and transport measurements under hydrostatic conditions showed at low temperatures and $P \sim 0.35$ GPa a sharp orthorhombic to collapsed tetragonal phase transition but no signature of superconductivity.[4] In contrast, recent neutron diffraction experiments on $CaFe_2As_2$ under uniaxial pressure along the c axis[5] indicate for pressures above 0.06 GPa and at low temperatures the presence of an intermediate nonmagnetic tetragonal phase between the magnetic orthorhombic and the nonmagnetic collapsed tetragonal phases. This phase was identified by the authors as the phase responsible for superconductivity at $T = 10$ K. Other reports based on muon spin-relaxation measurements suggest the existence of superconductivity in the orthorhombic phase, raising the question whether superconductivity and magnetism can coexist.[6]

$BaFe_2As_2$ shows an even more complex behavior under pressure. At ambient pressure it undergoes a phase transition from a metallic tetragonal phase to an orthorhombic antiferromagnetic phase at $T = 140$ K. Under pressure the gradual appearance of a superconducting dome has been observed by various groups[7] though the role of nonhydrostatic conditions is not yet well understood.[8] Recent synchrotron x-ray diffraction experiments under pressure[9] observe at $T = 300$ K a tetragonal to collapsed tetragonal phase transition at $P = 22$ GPa under hydrostatic conditions, while this transition appears already at $P = 17$ GPa under nonhydrostatic conditions. On the other hand, the authors of Ref. 10 find at a lower temperature of $T = 33$ K that $BaFe_2As_2$ undergoes a phase transition from a magnetic orthorhombic to a nonmagnetic collapsed tetragonal phase at $P = 29$ GPa and report an anomaly in the As-Fe-As bond angles at 10 GPa that they ascribe to be of electronic origin. In contrast, high-pressure neutron diffraction experiments[11] performed at $T = 17$ K find a tetragonal phase at 3 and 6 GPa.

These experimental results show that the onset of superconductivity as well as the appearance of several structural phases at low temperatures in $CaFe_2As_2$ and $BaFe_2As_2$ are extremely sensitive to the pressure conditions[5,12–14] and are a subject of intensive debate. In view of this strong controversy we present *ab initio* density functional theory results for the electronic, magnetic, and structural behavior of both systems under uniaxial and hydrostatic pressure conditions. Previous theoretical approaches which have examined the properties of the 122 family under hydrostatic pressure have employed either fixed volume structural optimizations[15] or molecular dynamics[16] Recently, anisotropic pressure studies on $BaFe_2As_2$ based on ground state geometry calculations of more than 300 structures at different fixed volumes were reported in Ref. 17. Our approach consists of constant pressure structural relaxations which allows us to probe the low-temperature portion of the phase diagram in a relatively simple and straightforward way. With this approach we can treat *nonhydrostatic* conditions which are at the heart of this work.

We find that uniaxial pressure along the c axis significantly reduces the transition pressures in both systems. $CaFe_2As_2$ shows for both pressure conditions an orthorhombic to collapsed tetragonal transition, though the transition is less abrupt when uniaxial pressure is applied. For $BaFe_2As_2$ we observe two phase transitions from orthorhombic to collapsed tetragonal through an intermediate nonmagnetic tetragonal phase. An analysis of the electronic band structure features near the critical pressures reveals the origin of the sensitivity of the systems to pressure conditions.

II. METHODS

Calculations were performed using the Vienna *ab initio* simulations package (VASP)[18] with the projector augmented wave (PAW) basis[19] in the generalized gradient approximation

(GGA). Structural relaxations under hydrostatic pressure were carried out with the conjugate gradient (CG) method as implemented in the VASP package. The energy cutoff was set to 300 eV and a Monkhorst-Pack uniform grid of $(6 \times 6 \times 6)$ points was used for the integration of the irreducible Brillouin zone. For relaxations with the CG algorithm two cycles were performed in order to minimize the error caused by the Pulay stress. Note that the reported bond compressions of up to 7% at 50 GPa do not affect the precision of the PAW basis. In order to perform relaxations under uniaxial pressure we modified the fast inertial relaxation engine[20] (FIRE) algorithm to be able to handle full structural relaxations with an arbitrary stress tensor.

III. $CaFe_2As_2$ RESULTS

In Fig. 1 we show the evolution of lattice parameters, volume, and Fe-Fe, Fe-As distances under hydrostatic and (c-axis) uniaxial pressure for $CaFe_2As_2$. We find a first-order phase transition from a magnetic (stripe order) orthorhombic phase to a nonmagnetic collapsed tetragonal phase at $P_c = 3.05$ GPa ($P_c = 0.48$ GPa) under hydrostatic (uniaxial) pressure and at zero temperature we do not observe any intermediate tetragonal phase under uniaxial stress.[5]

In hydrostatic conditions, a and b expand at the orthorhomic to collapsed tetragonal phase transition with b abruptly increasing in value, while c shows a significant collapse of 6.5% [Fig. 1(a)] and the unit cell volume shows a sharp drop of about 4.3% [Fig. 1(c)]. The sudden expansion of b can be explained as a consequence of the Pauli principle[16]: As long as an antiferromagnetically ordered moment exists in the orthorhombic phase, Fe $3d$ orbitals may overlap to some degree along the b direction, but in the paramagnetic state of the collapsed tetragonal phase, the same orbitals on neighboring Fe sites repel each other. The value of $c/a_t = 2.58$ with $a_t = a/\sqrt{2}$ indicates the onset of a collapsed tetragonal phase. Our results are in good qualitative agreement with experimental[3] observations, except for the overestimation of the critical pressure ($P_c^{\text{exp}} = 0.3$ GPa) also found in previous theoretical studies.[15,16] Following the changes of the lattice parameters at P_c, the in-plane Fe-Fe distances show a sharp increase at P_c while the out-of-plane Fe-As distance decreases [Fig. 1(e)]. Using the generalized Birch-Murnaghan $p - V$ equation of state[21] we obtained a bulk modulus $B = 70 \pm 3$ GPa at ambient pressure, while at P_c the bulk modulus jumps from 56 ± 3 to 105 ± 2 GPa. In order to obtain these estimates we performed a series of fits for every phase separately considering every pressure point of our data as a reference pressure. In this way we obtain the bulk modulus as a function of pressure.

In contrast to the hydrostatic case, when uniaxial pressure is applied [Fig. 1(b)] the a and b lattice parameters expand significantly while c is compressed up to $P_c = 0.48$ GPa where a drop for c is observed while a and b continue to expand monotonously. The volume reduces by 3.4% and the ratio $c/a_t = 2.56$ at P_c [Fig. 1(c)] denotes the entrance to a collapsed tetragonal phase, where magnetism is suppressed completely. The phase transition shifts to smaller P_c compared to hydrostatic pressure, which is in very good agreement with experiments under nonhydrostatic pressure conditions.[5] Nevertheless, the authors of Ref. 5 find for pressures above 0.06 GPa a stabilization of the high-temperature tetragonal structure down to temperatures below the superconducting transition. This phase is not seen in our calculations which may be related to the fact that at very low temperatures the tetragonal phase may be disappearing again (Fig. 1 of Ref. 5).

In order to understand the differences in behavior observed between the hydrostatic and uniaxial pressures, we show in Fig. 2 the orbital weighted band structure and $k_z = 0$, $k_y = 0$, and $k_x + k_y = 0$ Fermi surface cuts of $CaFe_2As_2$ under hydrostatic [Figs. 2(b) and 2(c)] and uniaxial pressure [Figs. 2(d) and 2(e)] at pressures below and above the phase transition. Band structures and Fermi surfaces were calculated using the full-potential local orbital (FPLO) basis.[22] The band structure and Fermi surface cuts at ambient pressure are also

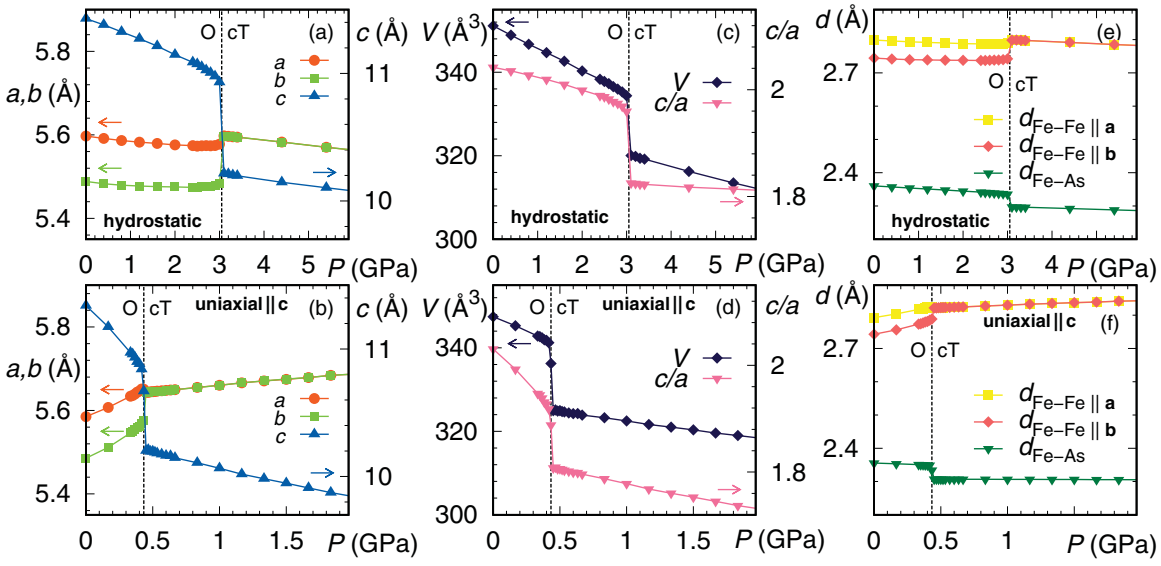

FIG. 1. (Color online) Structure of $CaFe_2As_2$ under hydrostatic and uniaxial pressure. Lattice parameters (a) and (b), volume and axis ratio (c) and (d), and selected bond lengths (e) and (f).

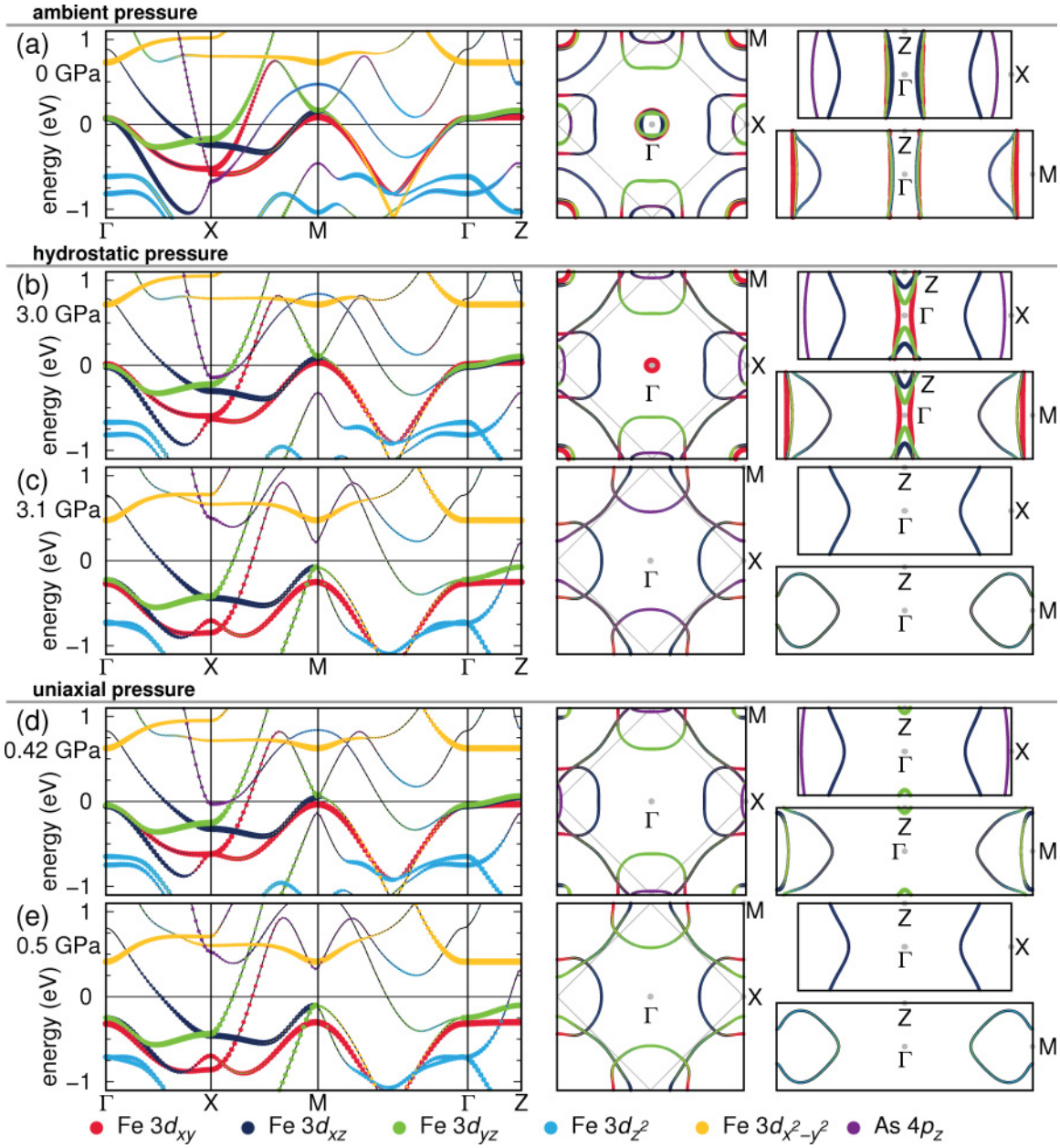

FIG. 2. (Color online) Band structure and $k_z = 0$, $k_y = 0$, and $k_x + k_y = 0$ Fermi surface cuts of $CaFe_2As_2$.[22] For the orbital character, x and y point along the nearest neighbor Fe-Fe connections.

shown for comparison [Fig. 2(a)]. We use the orthorhombic space group $Fmmm$ for all band structure plots in order to facilitate comparison. The behavior of the electronic structure in the vicinity of the Fermi energy is crucial for understanding the transition. Right below P_c both pressure conditions show a high density of Fe d_{xz}, d_{yz}, and d_{xy} states at E_F [see in Figs. 2(b) and 2(d) the Γ-Z path and near M] which are pushed away above P_c [Figs. 2(c) and 2(e)] and the hole pockets at Γ disappear, suppressing possible nesting conditions. The compression along c enforces the interlayer As p_z-As p_z bonding[23] which can be related to the proximity of the As p_z band to E_F near P_c. Uniaxial stress is for this process more effective than hydrostatic pressure since a similar electronic behavior is reached at much smaller pressures as observed in Figs. 2(d) and 2(e). In agreement with Ref. 24 the collapsed tetragonal phase sets in as soon as the Fe magnetic moment goes to zero. Note that the changes in the electronic structure at the phase transition in the uniaxial pressure case [Figs. 2(d) and 2(e)] are more subtle than for hydrostatic pressure, in agreement with the somewhat less abrupt change of the lattice as shown in Figs. 1(b), 1(d), and 1(f).

Also, the shape of the Fermi surface derived from Fig. 2 in the collapsed tetragonal phase agrees well with the de Haas van Alphen measurements performed for $CaFe_2P_2$ ($c/a_t = 2.59$), where a highly dispersive topology in the c axis as well as the absence of the hole pocket at the Γ point has been reported[25] [compare Figs. 2(c) and 2(e) with Figs. 2 and 3 of Ref. 25]. The isoelectronic substitution of As by P in

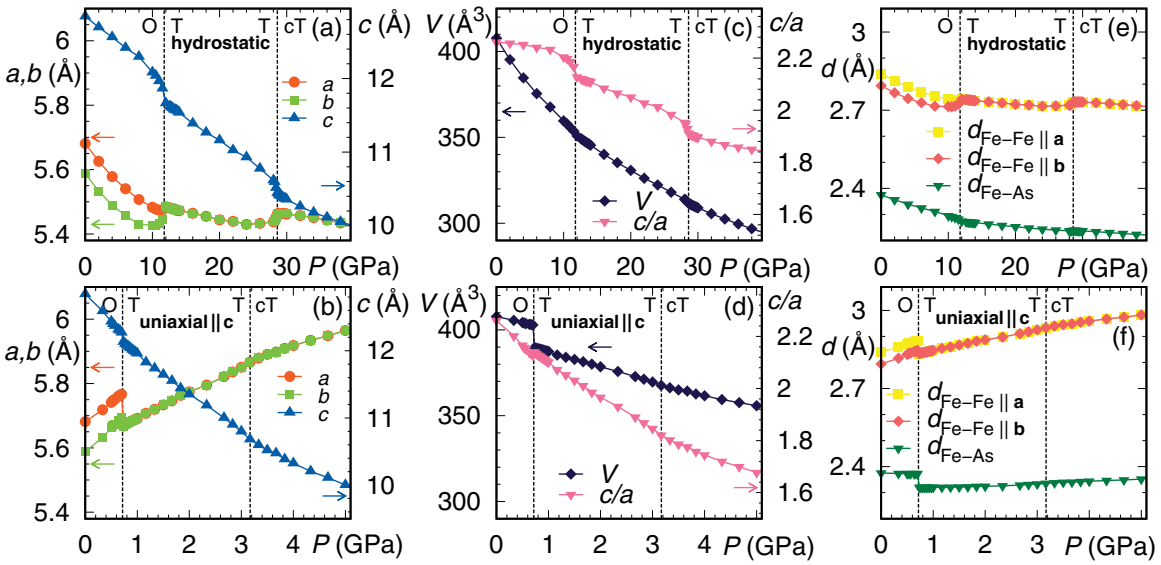

FIG. 3. (Color online) Structure of $BaFe_2As_2$ under hydrostatic and uniaxial pressure. Lattice parameters (a) and (b), volume and axis ratio (c) and (d), and selected bond lengths (e) and (f).

$CaFe_2As_2$ corresponds to application of chemical pressure and shows similar features to the collapsed tetragonal phase of $CaFe_2As_2$ obtained after application of (hydrostatic) pressure. The similarity of chemical pressure and applied pressure has already been discussed in Refs. 25 and 11. In fact, comparison of our obtained $c/a_t = 2.58$ ratio and As position $z_{As} = 0.1358$ (hydrostatic) in the collapsed tetragonal phase of $CaFe_2As_2$ with the measured $c/a_t = 2.59$ and P position $z_P = 0.1357$ of $CaFe_2P_2$ shows the high resemblance between both crystal structures.

IV. $BaFe_2As_2$ RESULTS

We now proceed with the analysis of $BaFe_2As_2$. In Fig. 3 we present the changes in lattice parameters, volume, and atomic distances under hydrostatic and uniaxial pressures for $BaFe_2As_2$. Similar to $CaFe_2As_2$, the critical pressures under uniaxial stress are reduced with respect to hydrostatic conditions. This observation was also reported by recent constant volume density functional theory calculations on $BaFe_2As_2$ under nonhydrostatic pressure.[17] $BaFe_2As_2$, contrary to $CaFe_2As_2$, shows two phase transitions. At $P_{c_1} = 11.75$ GPa ($P_{c_1} = 0.72$ GPa) we find a phase transition from an antiferromagnetic orthorhombic to a nonmagnetic tetragonal phase under hydrostatic (uniaxial) conditions. A second smooth phase transition to a collapsed tetragonal phase is obtained for $P_{c_2} = 28.6$ GPa ($P_{c_2} = 3.17$ GPa) [Figs. 3(c) and 3(d)].[9] High-pressure neutron diffraction experiments[11] as well as previous theoretical calculations under hydrostatic pressure conditions also find a phase transition to an intermediate tetragonal phase[15,16] but recent synchrotron x-ray diffraction experiments under nonhydrostatic conditions see no signature of an intermediate tetragonal phase at low temperatures. Nevertheless, an anomaly in the As-Fe-As bond angles at $P \sim 10$ GPa (Ref. 10) as well as a loss of magnetic moment[14] have been reported. This could be related to the phase transition that we find at $P_{c_1} = 11.75$ GPa where magnetism is suppressed. At higher pressures the agreement of the onset of the collapsed tetragonal phase with the x-ray diffraction data[10] is very good. Clearly the phase transitions in $BaFe_2As_2$ are less abrupt than in $CaFe_2As_2$. The ambient pressure bulk modulus is estimated at 67 ± 4 GPa, in good agreement with experimentally reported values[10] of 82.9 ± 1.4 and 65.7 ± 0.8 GPa at 33

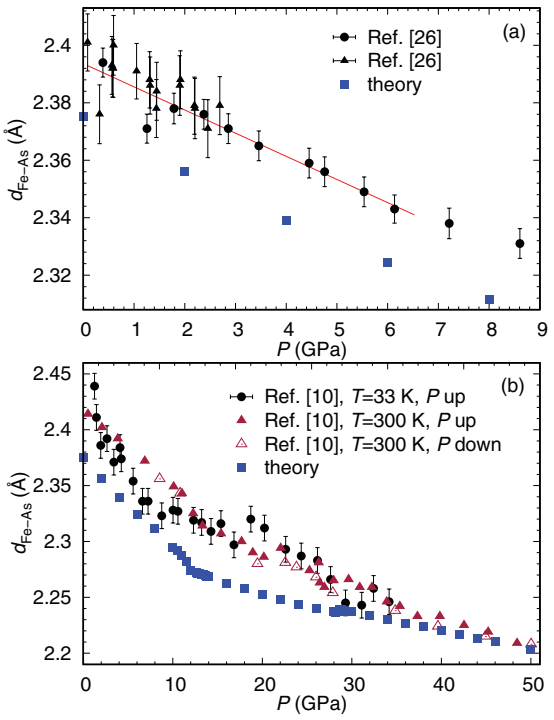

FIG. 4. (Color online) Comparison of $T = 0$ calculated (squares) and measured Fe-As bond distances in $BaFe_2As_2$ as a function of pressure. (a) $d_{Fe\text{-}As}$ from XAFS experiment at $T = 298$ K (triangles, circles).[26] (b) $d_{Fe\text{-}As}$ from x-ray diffraction at $T = 33$ K (circles) and $T = 300$ K (triangles).[10] P up and down indicate application and release of pressure.

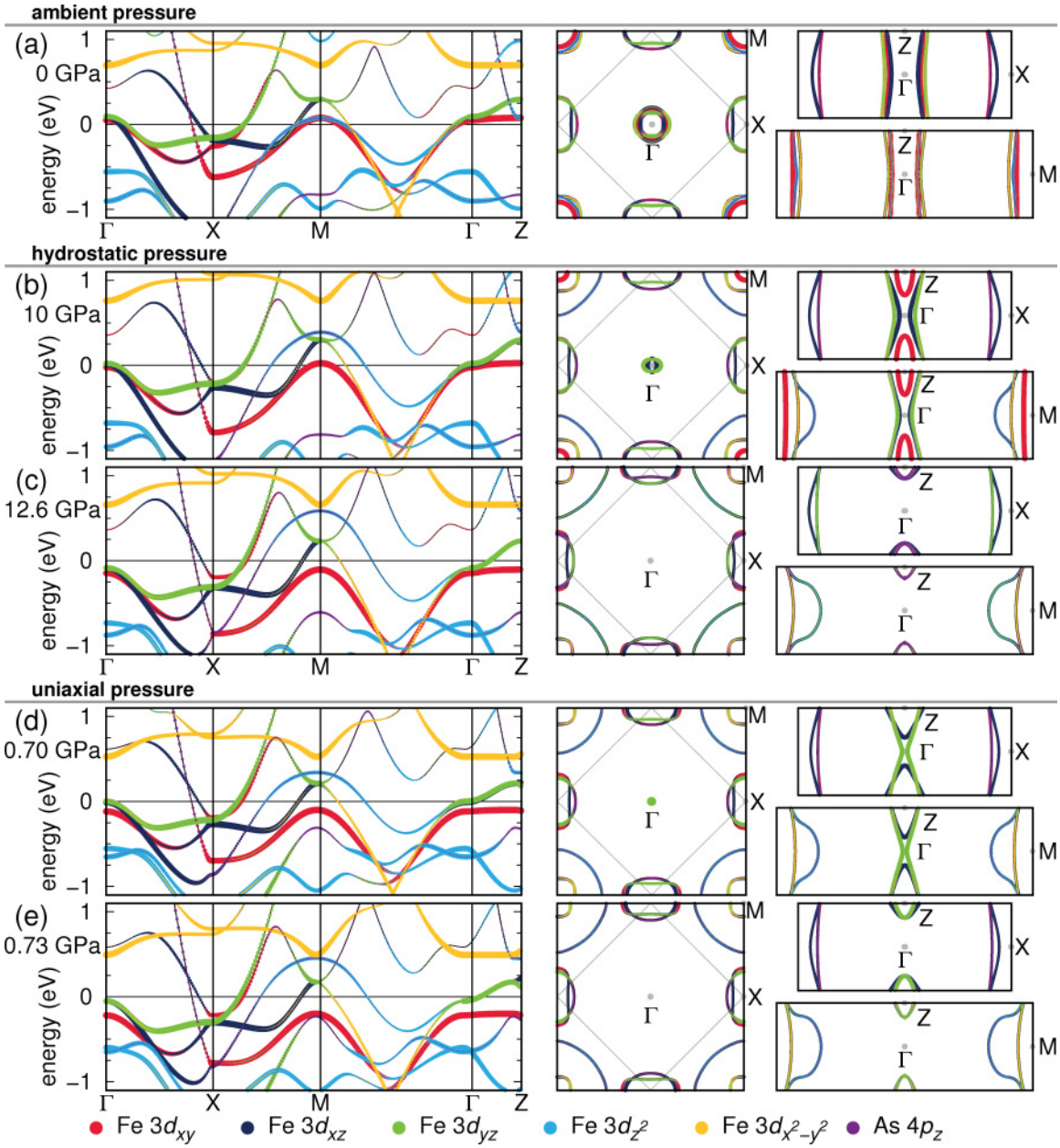

FIG. 5. (Color online) Band structure and $k_z = 0$, $k_y = 0$, and $k_x + k_y = 0$ Fermi surface cuts of $BaFe_2As_2$.[22]

and 300 K, respectively. At P_{c_1}, the bulk modulus abruptly increases from 98 ± 4 to 128 ± 3 GPa and at P_{c_2} it jumps from 150 ± 3 to 173 ± 2 GPa. This is in very good agreement with the experimental estimate of $B = 153 \pm 3$ GPa for the collapsed tetragonal phase.[10] We also analyzed the Fe-As bond compressibility for $P = 9$ GPa (hydrostatic) and found $\kappa = 3.5 \times 10^{-3}$ GPa^{-1} which is in excellent agreement with $\kappa = 3.3 \times 10^{-3}$ GPa^{-1} obtained in an extended x-ray absorption fine structure (EXAFS) experiment.[26] In Fig. 4(a) we show the comparison of the measured pressure dependence of the Fe-As bond distances[26] with our results. Due to different temperatures (experiment is performed at room temperature, theory at $T = 0$) our distances are shorter by about 0.02 Å (0.8%), but the overall agreement is good. In Fig. 4(b) we show the comparison to the x-ray diffraction measurement of the Fe-As bond distances[10] over a large pressure range. The comparison is particularly good at low and at high pressures; in the tetragonal phase (11.75 to 28.6 GPa) the deviations are a bit larger.

In Fig. 5 we present the orbital weighted band structure and $k_z = 0$, $k_y = 0$, and $k_x + k_y = 0$ Fermi surface cuts of $BaFe_2As_2$ under hydrostatic [Figs. 5(b) and 5(c)] and uniaxial pressure conditions [Figs. 5(d) and 5(e)] at two pressures below and above the orthorhombic to tetragonal phase transition at $P_{c_1} = 11.75$ GPa ($P_{c_1} = 0.72$ GPa). Similar to $CaFe_2As_2$ we observe below P_{c_1} a high density of Fe d_{xz}, d_{yz}, and d_{xy} states at E_F which is pushed down (less drastically than in $CaFe_2As_2$) for pressures above P_{c_1}. The hole pockets disappear at the Γ point and the Fe magnetic moment goes to zero. Here the As p_z band seems to be little affected at the critical pressure. In contrast, at $P_{c_2} = 28.6$ GPa ($P_{c_2} = 3.17$ GPa) (band structure not shown) the As p_z band is pushed toward the Fermi level

indicating a strong As p_z-As p_z bonding while entering the collapsed tetragonal phase. These results show that under perfect hydrostatic or perfect uniaxial pressure conditions neither the intermediate tetragonal phase nor the collapsed tetragonal phase fulfill Fermi surface nesting conditions. In fact, we find that the structural parameters measured in Ref. 11 are similar to our calculated parameters far below P_{c_1} in the orthorhombic phase (except for the orthorhombic distortion), where well defined hole pockets are found at the Γ point.

V. CONCLUSIONS

In summary, we have presented finite pressure density functional theory calculations which allow the investigation of *nonhydrostatic* pressure conditions. Our finite pressure relaxed structures show good agreement with the available experimental data (volume, bond lengths, and compressibilities) though our magnetic moments in the orthorhombic phase are larger than the observed experimental values. We expect that this overestimation affects mostly the values of P_c. Comparison of our calculated Fe-As bond distances at different pressures with measured distances[26] shows good agreement. Also, available de Haas van Alphen measurements performed for $CaFe_2P_2$[25] agree well with our predicted Fermi surface shapes for $CaFe_2As_2$ in the collapsed tetragonal phase. This overall agreement with experimental observations demonstrates that the presented constant pressure calculations provide a reliable theoretical prediction of structures under nonhydrostatic pressure conditions, allowing for arbitrary stress tensors in future studies. Such calculations can complement experiments and help identify the precise degree of hydrostaticity. We find that uniaxial stress along the c axis considerably reduces the critical pressures for $CaFe_2As_2$ and $BaFe_2As_2$. This behavior can be understood by the fact that the phase transitions are strongly dictated by the electronic properties in the vicinity of the Fermi energy, as shown by our electronic structure analysis. While $CaFe_2As_2$ undergoes a magnetic orthorhombic to a nonmagnetic collapsed tetragonal phase for both pressure conditions and no indication of an intermediate tetragonal phase is observed under uniaxial stress, $BaFe_2As_2$ shows two phase transitions from a magnetic orthorhombic to a collapsed tetragonal phase through an intermediate nonmagnetic tetragonal phase for both pressure conditions. All nonmagnetic phases show a disappearance of the hole pockets at the Γ point suppressing possible Cooper pair scattering channels between electron and hole pockets. Such scattering channels have been discussed to be important for the superconductivity in $BaFe_2As_2$.[27] More experiments need to be done in order to understand the origin of the superconducting phase observed in these materials under various pressure conditions.

ACKNOWLEDGMENTS

We would like to thank A. I. Coldea for useful discussions, the Deutsche Forschungsgemeinschaft for financial support through Grant SPP 1458, the Helmholtz Association for support through HA216/EMMI and the center for scientific computing (CSC, LOEWE-CSC) in Frankfurt for computing facilities.

[1] Y. Kamihara, T. Watanabe, M. Hirano, and H. Hosono, J. Am. Chem. Soc. **130**, 3296 (2008).
[2] M. S. Torikachvili, S. L. Bud'ko, N. Ni, and P. C. Canfield, Phys. Rev. Lett. **101**, 057006 (2008).
[3] A. Kreyssig, M. A. Green, Y. Lee, G. D. Samolyuk, P. Zajdel, J. W. Lynn, S. L. Bud'ko, M. S. Torikachvili, N. Ni, S. Nandi, J. B. Leão, S. J. Poulton, D. N. Argyriou, B. N. Harmon, R. J. McQueeney, P. C. Canfield, and A. I. Goldman, Phys. Rev. B **78**, 184517 (2008).
[4] W. Yu, A. A. Aczel, T. J. Williams, S. L. Bud'ko, N. Ni, P. C. Canfield, and G. M. Luke, Phys. Rev. B **79**, 020511 (2009).
[5] K. Prokeš, A. Kreyssig, B. Ouladdiaf, D. K. Pratt, N. Ni, S. L. Bud'ko, P. C. Canfield, R. J. McQueeney, D. N. Argyriou, and A. I. Goldman, Phys. Rev. B **81**, 180506 (2010).
[6] T. Goko, A. A. Aczel, E. Baggio-Saitovitch, S. L. Bud'ko, P. C. Canfield, J. P. Carlo, G. F. Chen, P. Dai, A. C. Hamann, W. Z. Hu, H. Kageyama, G. M. Luke, J. L. Luo, B. Nachumi, N. Ni, D. Reznik, D. R. Sanchez-Candela, A. T. Savici, K. J. Sikes, N. L. Wang, C. R. Wiebe, T. J. Williams, T. Yamamoto, W. Yu, and Y. J. Uemura, Phys. Rev. B **80**, 024508 (2009).
[7] P. L. Alireza, Y. T. C. Ko, J. Gillett, C. M. Petrone, J. M. Cole, G. G. Lonzarich, and S. E. Sebastian, J. Phys. Condens. Matter **21**, 012208 (2009).
[8] J. Paglione and R. L. Greene, Nat. Phys. **6**, 645 (2010).
[9] W. Uhoya, A. Stemshorn, G. Tsoi, Y. K. Vohra, A. S. Sefat, B. C. Sales, K. M. Hope, and S. T. Weir, Phys. Rev. B **82**, 144118 (2010).
[10] R. Mittal, S. K. Mishra, S. L. Chaplot, S. V. Ovsyannikov, E. Greenberg, D. M. Trots, L. Dubrovinsky, Y. Su, Th. Brueckel, S. Matsuishi, H. Hosono, and G. Garbarino, Phys. Rev. B **83**, 054503 (2011).
[11] S. A. J. Kimber, A. Kreyssig, Y. Z. Zhang, H. O. Jeschke, R. Valenti, F. Yokaichiya, E. Colombier, J. Yan, T. C. Hansen, T. Chatterji, R. J. McQueeney, P. C. Canfield, A. I. Goldman, and D. N. Argyriou, Nat. Mater. **8**, 471 (2009).
[12] A. I. Goldman, A. Kreyssig, K. Prokeš. D. K. Pratt, D. N. Argyriou, J. W. Lynn, S. Nandi, S. A. J. Kimber, Y. Chen, Y. B. Lee, G. Samolyuk, J. B. Leão, S. J. Poulton, S. L. Bud'ko, N. Ni, P. C. Canfield, B. N. Harmon, and R. J. McQueeney, Phys. Rev. B **79**, 024513 (2009).
[13] T. Yamazaki, N. Takeshita, R. Kobayashi, H. Fukazawa, Y. Kohori, K. Kihou, C. H. Lee, H. Kito, A. Iyo, and H. Eisaki, Phys. Rev. B **81**, 224511 (2010).
[14] W. J. Duncan, O. P. Welzel, C. Harrison, X. F. Wang, X. H. Chen, F. M. Grosche, and P. G. Niklowitz, J. Phys. Condens. Matter **22**, 052201 (2010).
[15] N. Colonna, G. Profeta, A. Continenza, and S. Massidda, Phys. Rev. B **83**, 094529 (2011).
[16] Y.-Z. Zhang, H. C. Kandpal, I. Opahle, H. O. Jeschke, and R. Valentí, Phys. Rev. B **80**, 094530 (2009).

[17]N. Colonna, G. Profeta, and A. Continenza, Phys. Rev. B **83**, 224526 (2011).

[18]G. Kresse and J. Hafner, Phys. Rev. B **47**, 558 (1993); G. Kresse and J. Furthmüller, *ibid*. **54**, 11169 (1996); Comput. Mater. Sci. **6**, 15 (1996).

[19]P. E. Blöchl, Phys. Rev. B **50**, 17953 (1994); G. Kresse and D. Joubert, *ibid*. **59**, 1758 (1999).

[20]E. Bitzek, P. Koskinen, F. Gähler, M. Moseler, and P. Gumbsch, Phys. Rev. Lett. **97**, 170201 (2006).

[21]N. Sata, G. Shen, M. L. Rivers, and S. R. Sutton, Phys. Rev. B **65**, 104114 (2002).

[22]K. Koepernik and H. Eschrig, Phys. Rev. B **59**, 1743 (1999); [http://www.FPLO.de].

[23]D. Johrendt, C. Felser, O. Jepsen, O. K. Andersen, A. Mewis, and J. Rouxel, J. Solid State Chem. **130**, 254 (1997).

[24]T. Yildirim, Phys. Rev. Lett. **102**, 037003 (2009).

[25]A. I. Coldea, C. M. J. Andrew, J. G. Analytis, R. D. McDonald, A. F. Bangura, J.-H. Chu, I. R. Fisher, and A. Carrington, Phys. Rev. Lett. **103**, 026404 (2009).

[26]E. Granado, L. Mendonça-Ferreira, F. Garcia, G. deM. Azevedo, G. Fabbris, E. M. Bittar, C. Adriano, T. M. Garitezi, P. F. S. Rosa, L. F. Bufaiçal, M. A. Avila, H. Terashita, and P. G. Pagliuso, Phys. Rev. B **83**, 184508 (2011).

[27]S. Graser, A. F. Kemper, T. A. Maier, H.-P. Cheng, P. J. Hirschfeld, and D. J. Scalapino, Phys. Rev. B **81**, 214503 (2010).